NEW METHOD OF MPPT APPLICATION FOR DUAL-STAGE INVERTERS

Marcio Mendes Casaro
Federal University of Technology - Paraná
Av. Monteiro Lobato, km 04
Post Code: 84.016-210
Ponta Grossa, Paraná - Brazil
casaro@utfpr.edu.br

Denizar Cruz Martins
Power Electronics Institute
Federal University of Santa Catarina
P.O. Box 5119, Post Code: 88.040-970
Florianópolis, Santa Catarina - Brazil
denizar@inep.ufsc.br

***Abstract* – This paper presents a PV grid-connected system constructed with a three-phase dual-stage inverter. The dual-stage inverter tracks the maximum power operating point (MPOP) through a technique of maximum power point tracking (MPPT) that uses perturbation and observation algorithm (P&O) to maximize the inverter output power. The inverter direct axis current is used. The DC-DC converter operates with constant duty cycle and frequency. In addition, it has behavior matching that of the photovoltaic array. This characteristic allows indirect MPPT application. The variables in the inverter stage to control the grid current are the same used in the MPPT, therefore, any additional acquisitions are necessary. The isolation is performed by a high-frequency transformer becoming the system most compact. The simulation of a 12kW three-phase system discloses a fast dynamics and extremely efficient tracking.**

***Keywords* - Dual-stage inverter, high-frequency transformer, MPPT, P&O method.**

I. INTRODUCTION

The photovoltaic solar energy represents an emergent technology in function of the continuous fall in the production costs and in the technological progress of the PV modules. This alternative energy can significantly contribute with the reduction in the emission of greenhouse gases in the atmosphere, which attack the environment deeply.

Around 75% of the PV systems installed in the world are grid connected [1]. These systems need an inverter that, depending on its topology, can be classified as presented to follow.

- Single-stage inverter: in one processing stage handle all tasks such as MPPT and the grid-current control.
- Dual-stage inverter: a DC-DC converter performs the MPPT and the inverter is responsible for controlling of the grid-current.
- Multistage inverter: various DC-DC converters are used, which are responsible for the MPPT, and only one inverter takes care of the grid-current control.

In order to provide galvanic isolation between the grid and photovoltaic modules, the inverter, traditionally, is equipped with low-frequency transformer, which is weighed, great, expensive and present low efficiency. By replacing the low with a high-frequency transformer, the efficiency can be increased by 2% [1]. For powers above 750W, the Full-Bridge converter normally is used to perform the MPPT and isolation [2]. This reference also indicates the centralization of the inverter so that the costs of the system are reduced. This type of project foresees that in all the plant will have only one inverter to which will be connected the photovoltaic modules, in series and parallel, according to Figure 1.

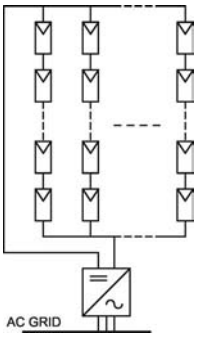

Fig. 1. Centralized inverter architecture.

From the context previously presented, this paper proposes a dual-stage inverter to operate according Figure 1, however, with two basic differences.

1º) Uses a three-phase DC-DC converter in place of a single-phase. In [3] is demonstrated that the three-phase conversion has some advantages such as:

- High-frequency transformer reduction in comparison to the transformer used in a Full-Bridge converter, operating with the same switching frequency.
- Increase of three times in the input and output current frequencies, reducing the size of the filters components.
- Better distribution of the losses.

2º) The MPPT is performed by the inverter. It is not acted on the control parameter of DC-DC converter, which operates with constant frequency and duty cycle. It is important to emphasize that any measurements of voltage or current in the photovoltaic array are made. It is an indirect MPPT, possible due the behavior matching between the DC-DC converter output I-V characteristic and the PV array I-V characteristic, when they are connected. Then, behavior matching serves as fundamental feature for DC-DC converters to reproduce the PV array I-V characteristic without control action.

The inverter perform the MPPT through the P&O method to maximize the direct axis current, Id, required for the grid current control. The current Id reflects the power delivered by the photovoltaic array and is expressed through the inverter modeling, using the Park transformation. Then, the inverter output power is maximized without additional senses. In a single-stage inverter, this principle also can be used.

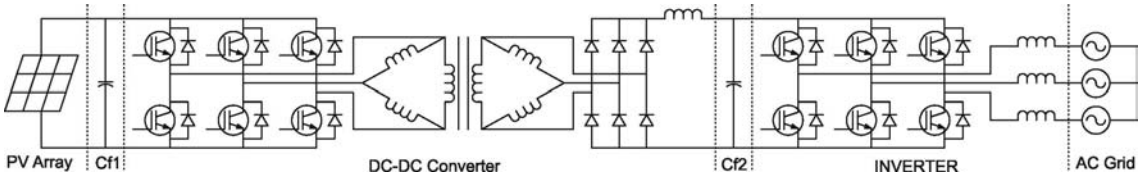

Fig. 2. Dual-stage inverter topology.

Figure 2 presents the proposal topology for the dual-stage inverter.

II. PHOTOVOLTAIC ARRAY MODELING

The proposed MPPT is based on the behavior of the photovoltaic array by means of temperature and irradiation variations. Thus, the mathematical model of the PV cells is implemented in the form of a current source controlled by voltage, sensible to two input parameters, that is, temperature (ºC) and solar irradiation power (W/m^2).

An equivalent simplified electric circuit of a photovoltaic cell is presented in Figure 3.

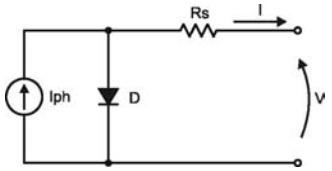

Fig. 3. Equivalent electric circuit of a simplified single-diode model (SSDM) of a PV solar cell.

Although it is a simplified version, this equivalent circuit is enough to represent different types of photovoltaic cells when the temperature effects are considered [4]. From [5], it is verified that the cells of polycrystalline material are contemplated. This material is distinguished because information gotten of datasheet of a polycrystalline module are used in the simulation studies, however, the relevant aspects for the control, shown from the model, are not only applied to this type of material.

In a more complete version, the equivalent circuit of Figure 3 has two electrical resistors, Rs and Rp. According to [6] and [7], both resistors can be neglected. However, it is demonstrated that the series resistor, Rs, has a great impact on the inclination of the I-V characteristic curve, becoming it more accurate between the maximum power operating point and the open circuit voltage. This information can also be found in [8].

Expression (1) can be obtained from Figure 3.

$$I = Iph - Ir \cdot \left[e^{q \cdot (V + I \cdot Rs)/n \cdot k \cdot T} - 1 \right] \quad (1)$$

Where:
V, I - voltage and current across the cell;
Iph - photocurrent;
Ir - cell reverse saturation current;
q - charge of an electron;
Rs - intrinsic series resistance of the cell;
n - ideality factor of the p-n junction;
k - Boltzmann's constant;
T - temperature.

Photocurrent depends on the solar irradiation and the temperature.

$$Iph = \left[Isc + \alpha \cdot (T - Tr) \right] \cdot \frac{Psun}{1000} \quad (2)$$

Where:
Isc - short-circuit current;
α - temperature coefficient of the short-circuit current;
Tr - reference temperature, for standard condition;
Psun - irradiance level. The standard power is 1000W/m^2.

The reverse saturation current varies according to the temperature.

$$Ir = Irr \cdot \left(\frac{T}{Tr} \right)^3 \cdot e^{\left[\frac{q \cdot E_G}{n \cdot k} \cdot \left(\frac{1}{Tr} - \frac{1}{T} \right) \right]} \quad (3)$$

Where:
Irr - cell reference reverse saturation current;
E_G - band-gap energy of the semiconductor used in the cell.

These equations can be found in [6] and [9]. The solution of (1) takes the characteristic curve for only one photovoltaic cell. However, the model is such that, if connected in a PV array form, it can be treated as only one cell with multiple associations in series and parallel [8]. Thus, the photovoltaic array, corresponding to ten parallel-connected strings, is simulated. Each string contains twenty four modules, which approximately produce the desired operation voltage of 400V. Therefore, it is found a 12kWp array formed by 240 KC50 modules from Kyocera. Figures 4 and 5 reflect the behavior obtained with the PV array model which is connected to DC-DC converter.

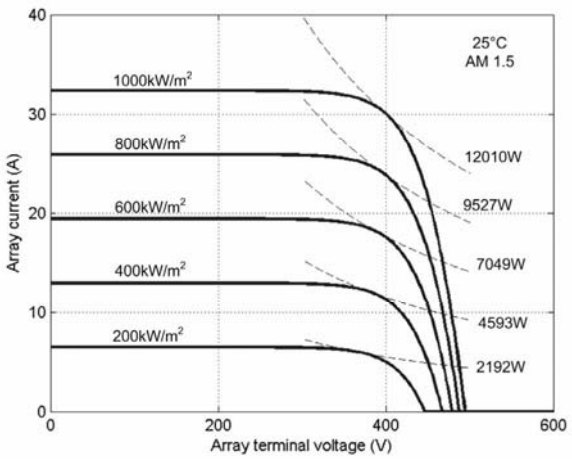

Fig. 4. Current-Voltage characteristics of photovoltaic array at various irradiance levels.

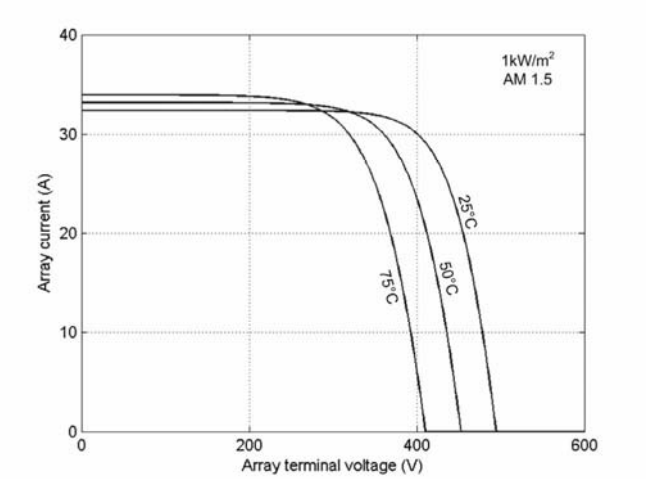

Fig. 5. Current-Voltage characteristics of photovoltaic array at various temperatures.

III. DC-DC CONVERTER

For powers above 10kW, single-phase DC-DC converters, as the Full-bridge, presents a severe stress in its components. In the three-phase topologies this stress is reduced and the performance is improved substantially, including the dynamics behavior, with faster response times [3]. Figure 6 shows a classical topology, which use high-frequency three-phase transformer in the DC-DC conversion.

In this Figure the transformer is replaced by the leakage inductances, which are very important to the operation and the mathematical analysis of the structure.

Figure 7 illustrates Iin and Vo in a switching period. All transistors conduct between 60° and 120°, defining the minimum and maximum converter duty cycle.

The leakage inductance (Ld) limits dIn/dt, affecting the value of the output voltage. The relation between these variables is express in (4).

$$Iin_{av} = Ia = \frac{Vo_{av}}{6 \cdot fs \cdot Ld} \cdot \left[(6 \cdot D - 1) - \frac{Vo_{av}}{Vin} \right] \qquad (4)$$

Where:
Iin_{av} - average input current;
Ia - array current;
Vo_{av} - average output voltage in the three-phase bridge rectifier;
fs - switching frequency;
D - duty cycle;
Vin - converter input voltage.

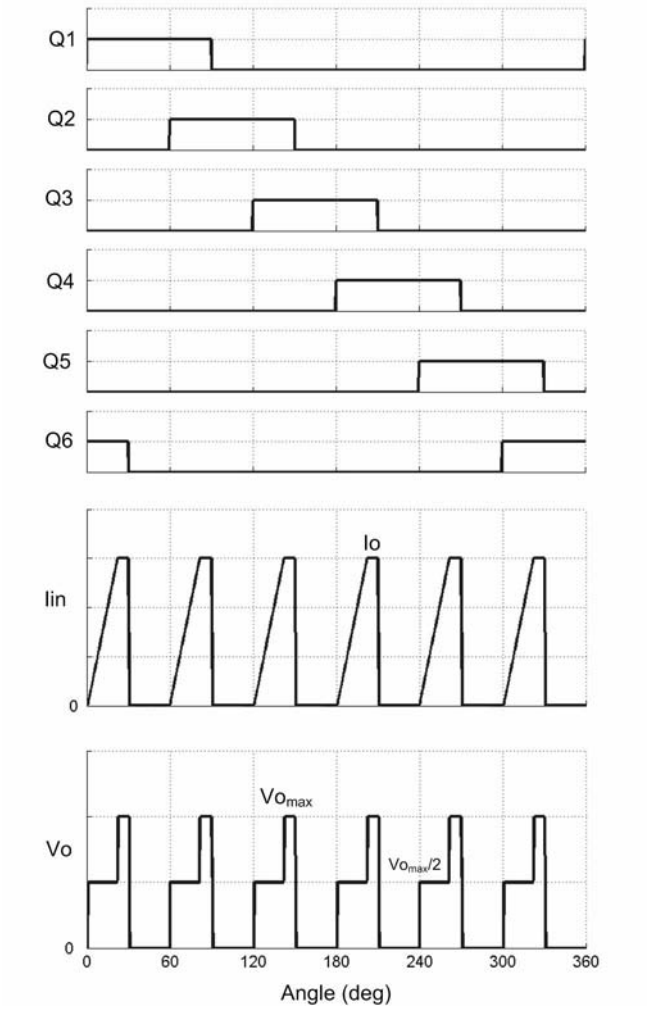

Fig. 7. Gate trigger pulses, input current and output voltage, in a switching period.

The validity of (4) is conditioned by (5).

$$Ld \le \frac{Vin}{12 \cdot fs \cdot Io_{av}} \cdot (6 \cdot D - 1) \qquad (5)$$

Where Io_{av} is the output average current of the converter.

From (5) the maximum value of Ld is directly proportional to D. To allow that the leakage inductance is restricted to the amplest range of possible values, D is chosen 1/3. In Figure 7, even with the maximum duty cycle, the gating signals of one arm are intercalated by intervals of 60º, that is, the dead time is naturally introduced by the converter operation mode, which confers extreme robustness.

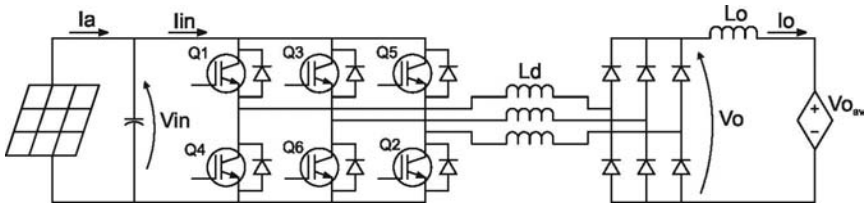

Fig. 6. DC-DC three-phase PWM converter.

With D = 1/3, the value of the inductance Lo is defined by (6).

$$Lo = Ld \cdot \frac{Io_{av}}{\Delta Io} \cdot \left(2 \cdot \frac{Vo_{av}}{Vin} - 1 \right) \quad (6)$$

Where ΔIo is the ripple of the converter output current.

In the proposal MPPT strategy, the voltage Vo_{av} is adjusted by the inverter periodically. Irradiations variations can occur between two adjusts. The positions taken for the MPOP in some irradiation levels form an almost vertical line, as presents the Figure 8. However, this overlapping line to the array I-V characteristic was not drawn by the union of the MPOPs, but through the equation (4), that is, it is the DC-DC converter input characteristic. In the horizontal axel is the voltage Vin and Iin_{av} is in the vertical axel. The variables and parameter used in the tracing are: Vo_{av} = 360V; fs = 20kHz; Ld = 10µH; D = 1/3.

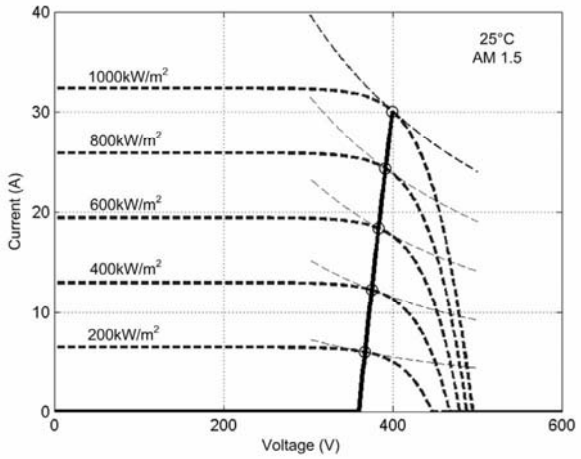

Fig. 8. DC-DC converter input characteristic, in solid line. The crossing of this line with the photovoltaic array I-V characteristic is distinguished.

Through the irradiance variations, the array operation point is defined by the crossing of its respective I-V characteristic curve with the converter input characteristic. How nearest this crossing will be of the MPOP lesser will be the relative tracking error, presented in (8).

IV. INVERTER

The temperature and the solar irradiation in the PV array modules vary in different way. The clouds movement can result in brusque alterations in the irradiance level. However, the temperature tends to vary much more slowly. Since temperature remains constant does not have necessity of the inverter intervention, whose task is to keep the voltage Vo clamped in a reference.

However, periodically, the inverter, through a P&O algorithm, regulates the value of Vo_{av} in order to shift the DC-DC converter input characteristic, that can be crossing with the array I-V characteristic far from the MPOP due to a temperature variation, as illustrated in Figure 9. Other MPPT methods also can be tested.

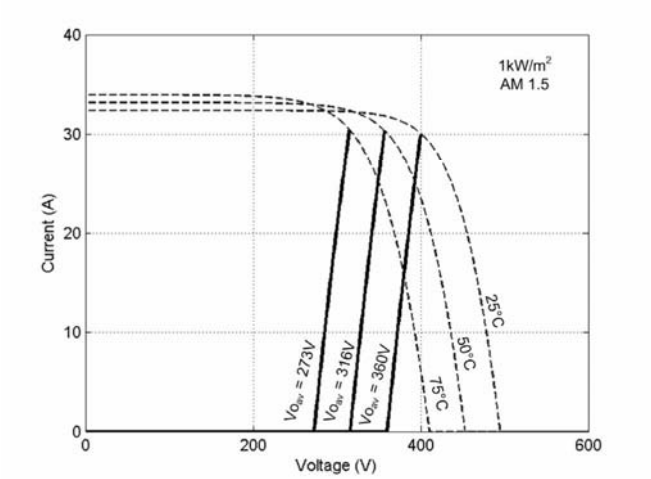

Fig. 9. Shifting of the DC-DC converter input characteristic due to the Vo_{av} adjustment by inverter.

The topology of the inverter is presented in Figure 10.

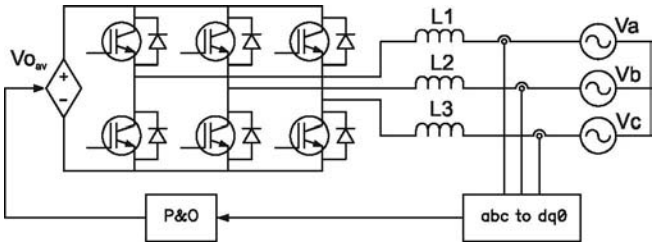

Fig. 10. Three-phase inverter.

Where Va, Vb and Vc are the AC grid phase voltages.

It is verified that P&O block is fed by a current obtained from Park transformation. It is about the direct axis current, Id. According to [10], the power that the inverter injects in the grid is given by $Pg = Vd \cdot Id$, where Vd is constant. Thus, the MPPT can be performed, perturbing Vo_{av} and observing Id. The Vo_{av} perturbation at the (k+1)-th sampling is given by (7).

$$\begin{aligned} & Vo_{av}\left((k+1)\cdot Ta\right) = Vo_{av}\left(k\cdot Ta\right) \pm \Delta V = \\ & = Vo_{av}\left(k\cdot Ta\right) + \left[Vo_{av}\left(k\cdot Ta\right) - Vo_{av}\left((k-1)\cdot Ta\right) \right] \cdot \\ & \cdot sign\left[Pg\left(k\cdot Ta\right) - Pg\left((k-1)\cdot Ta\right) \right] \end{aligned} \quad (7)$$

The efficiency of P&O method can be improved by the optimization of the sampling interval, Ta, and of the perturbation magnitude, ΔV.

The sampling interval must be as small as possible, without causing instability. Ta is chosen in accordance with the processor dynamics. Must be waited the system to reach the steady-state condition between two perturbations.

When the MPOP is found, after some iteration, the tracking algorithm provokes oscillations around this point until the clamping of the voltage Vo_{av}. It is desired that the Vo_{av} takes the system to act with the maximum efficiency. How much lesser will be the perturbation magnitude, more restricted will be the relative tracking error. However, the tracking of the MPOP is slower.

Beyond these, other recommendations can be found in [11] and [12].

V. SIMULATION RESULTS

Initially, the performance of the MPOP tracking when the voltage Vo_{av} and the temperature are kept constants is demonstrated. The relevant parameters and variables for this simulation are: Vo_{av} = 360V, fs = 20kHz, D = 1/3, Ld = 10µH, Lo = 240µH and Cf1 = 100µF.

Figure 11 presents the MPPT performance for fast atmospherics conditions changes. Table 1 shows the measured relative tracking error, defined in (8). It is possible to verify that the relative tracking error is very small. Thanks the behavior matching, to clamp Vo_{av} produce a similar result than to clamp Vin.

$$\varepsilon_R = \frac{P_{MPOP} - P_{MPPT}}{P_{MPOP}} \cdot 100\% \qquad (8)$$

Where:

P_{MPOP} - it is the maximum power that the photovoltaic array can supply, in the respective conditions of temperature and irradiation;

P_{MPPT} - it is the power obtained from the photovoltaic array using the proposal MPPT method.

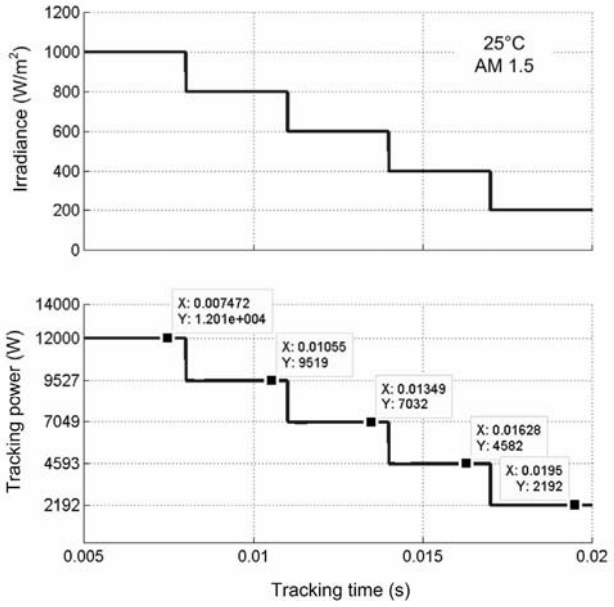

Fig. 11. MPPT performance for irradiation variation.

TABLE I
Relative tracking errors

Irradiance (W/m²)	P_{MPOP} (W)	P_{MPPT} (W)	ε_R (%)
1000	12010	12010	0
800	9527	9519	0.08
600	7049	7032	0.24
400	4593	4582	0.24
200	2192	2192	0

Figure 12 presents the voltage and the current in the terminals of the photovoltaic array connected to DC-DC converter. It is observed that the operation point is established by the converter input characteristic, in conformity to dashed line drawn through (4).

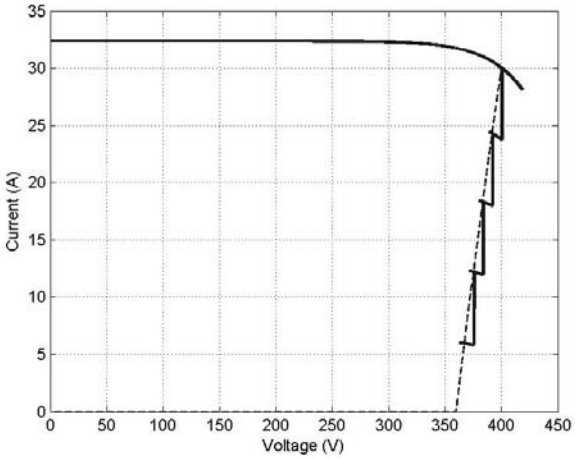

Fig. 12. Array terminal voltage and current behavior at various irradiance levels. DC-DC converter input characteristic in dashed line.

The MPOP shift an almost horizontal line when the temperature changes. Then, the intersection between the characteristics of PV array and DC-DC converter deviates of the MPOP, increasing the ε_R. In order to correct this problem, the P&O method is periodically to put in action in the inverter, as shown in Figure 13. The system uses a turns ratio transformer of 1:2, therefore the magnitude perturbation appear with 4V.

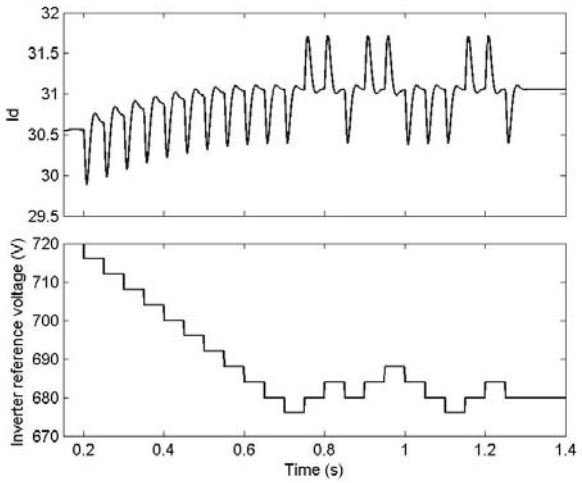

Fig. 13. Reference voltage perturbation and Id current observation.

With Ta = 50ms and ΔV = 2V, the MPPT performance is illustrated in Figure 14.

At 100ms, the temperature of the cells changes from 25ºC to 35ºC. The irradiance is 1kW/m² and the air mass is of 1.5.

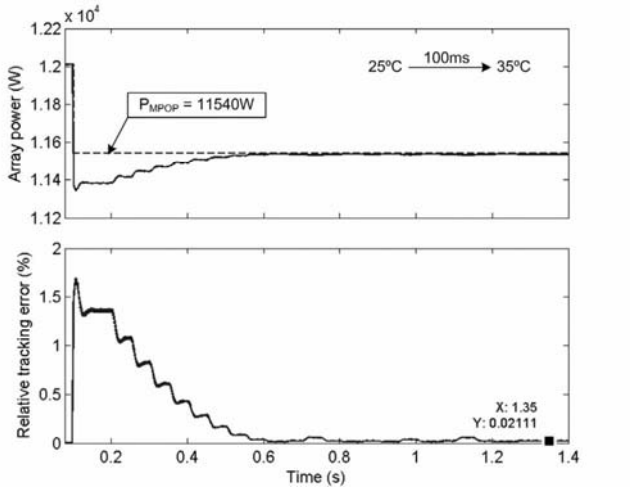

Fig. 14. MPPT performance for temperature variation.

VI. CONCLUSION

A new strategy of MPPT application was presented. Its application in powers above 10kW was considered, where three-phase systems present advantages on the single-phase ones. The topologies chosen for the converters qualify the dual-stage inverter studied to high power.

The transformer size can be minimized by the increase of the DC-DC converter switching frequency, which is independent that of the inverter stage.

Through the input characteristic of the three-phase DC-DC converter, which take its output to achieve a behavior matching that of the PV array, and the closed-loop control in the inverter stage, the tracking error obtained was insignificant.

The periodic action of the inverter prevents losses and instability, inherent problems of the P&O technique. When the MPOP is found the voltage Vo_{av} is clamped, avoiding voltage ripple in the photovoltaic array terminals. In this situation, the array operation point slide on the DC-DC converter input characteristic, near the MPOP, for fast atmospheric conditions changes.

The necessary variables to the grid-connected inverter control also were used in the MPPT, what becomes the structure cheapest. The inverter direct axis current was employed by the P&O algorithm.

REFERENCES

[1] X. Yuan and Y. Zhang, "Status and Opportunities of Photovoltaic Inverters in Grid-Tied and Micro-Grid Systems," *15th International Photovoltaic Science & Engineering Conference (PVSEC-15)*, pp. 226-227, 2005.

[2] J. M. Carrasco, L. G. Franquelo, J. T. Bialasiewicz, E. Galván, R. C. P. Guisado, M. A. M. Prats, J. I. León, and N. Moreno-Alfonso, "Power-Electronic Systems for the Grid Integration of Renewable Energy Sources: A Survey," *IEEE Transactions on Industrial Electronics*, vol. 53, no. 4, pp. 1002-1016, August 2006.

[3] P. D. Ziogas, A. R. Prasad, and S. Manias, "Analysis and Design of a Three-Phase Off-Line DC/DC Converter with High Frequency Isolation," *Proc. IAS'88 Conf*., pp. 813–820, 1988.

[4] W. Xiao, M. G. J. Lind, W. G. Dunford and A. Capel, "Real-Time Identification of Optimal Operating Points in Photovoltaic Power Systems," *IEEE Transactions on Industrial Electronics*, vol. 53, no. 4, pp. 1017-1026, August 2006.

[5] Y. Tsuno, Y. Hishikawa and K. Kurokawa, "Temperature and Irradiance Dependence of the I-V Curves of Various Kinds of Solar Cells," *15th International Photovoltaic Science & Engineering Conference (PVSEC-15)*, pp. 422-423, 2005.

[6] K.H. Hussein, I. Muta, T. Hoshino and M. Osakada, "Maximum Photovoltaic Power Tracking: an Algorithm for Rapidly Changing Atmospheric Conditions," *IEE Proc.-Gener. Transm. Distrib*., vol. 142, no 1, pp. 59-64, January 1995.

[7] N. Mutoh, M. Ohno and T. Inoue, "A Method for MPPT Control While Searching for Parameters Corresponding to Weather Conditions for PV Generation Systems," *IEEE Transactions on Industrial Electronics*, vol. 53, no. 4, pp. 1055-1065, August 2006.

[8] J. A. Gow and C. D. Manning "Development of a Photovoltaic Array Model for Use in Power Electronics Simulation Studies," *IEE Proceedings on Electric Power Applications*, vol. 146, no. 2, pp. 193-200, March 1999.

[9] C. Hua, J. Lin and C. Shen, "Implementation of a DSP-Controlled Photovoltaic System with Peak Power Tracking," *IEEE Transactions on Industrial Electronics*, vol. 45, no. 1, pp. 99-107, February 1998.

[10] D. Borgonovo, *Modeling and Control of Three-Phase PWM Rectifiers Using the Park Transformation (in Portuguese)*, Master's Thesis, Federal University of Santa Catarina, Florianópolis, 2001.

[11] N. Femia, G. Petrone, G. Spagnuolo and M. Vitelli, "Optimizing Duty-cycle Perturbation of P&O MPPT Technique," *35th Annual IEEE Power Electronics Specialists Conference*, pp. 1939-1944, 2004.

[12] N. Femia, G. Petrone, G. Spagnuolo and M. Vitelli, "Optimizing Sampling Rate of P&O MPPT Technique," *35th Annual IEEE Power Electronics Specialists Conference*, pp. 1945-1949, 2004.